Multiplicity Control in the Polygeminal Diazeniumdiolation of Active Hydrogen Bearing Carbons: Chemistry of a New Type of Trianionic Molecular Propeller

Navamoney Arulsamy and D. Scott Bohle*

Contribution from the Department of Chemistry, University of Wyoming, Laramie, Wyoming 82071-3838

Received July 17, 2000. Revised Manuscript Received May 11, 2001

Abstract: Over a century ago, Traube reported the reaction of four nitric oxides with acetone and sodium ethoxide to yield sodium methanebis(diazene-*N*-oxide-*N*′-hydroxylate) and sodium acetate. However, when this reaction is carried out in the presence of nitric oxide at slightly elevated pressures (35−40 psi), a product corresponding to the addition of six nitric oxides, sodium methanetris(diazene-*N*-oxide-*N*′-hydroxylate), forms as the main product in addition to a trace of the previously observed sodium methanebis(diazene-*N*-oxide-*N*′-hydroxylate) and sodium acetate. The corresponding potassium salts form when potassium hydroxide is employed as the base, while lithium hydroxide results in the formation of lithium methanebis(diazene-*N*-oxide-*N*′-hydroxylate) exclusively. Nitric oxide reacts with 3,3-dimethylbutan-2-one in the presence of sodium and potassium hydroxide in methanol to yield sodium and potassium 3,3-dimethylbutan-2-one-1,1,1-tris(diazene-*N*-oxide-*N*′-hydroxylate), respectively. In contrast, the reaction in the presence of lithium hydroxide forms lithium methanebis(diazene-*N*-oxide-*N*′-hydroxylate) and lithium pivalate. The differential reactivity of nitric oxide with acetone and 3,3-dimethylbutan-2-one in the presence of the three bases is attributed to competing hydrolytic reactions of the acetyl and trimethylacetyl group-containing intermediates. A mechanism is proposed for the nitric oxide addition to active methyl groups in these reactions, where the product distribution between the di- and trisubstituted methanes is under kinetic control of the competing reactions. The products are characterized by NMR and IR spectroscopy, differential scanning calorimetry, and elemental analysis. Two differentially hydrated forms of potassium methanetris(diazene-*N*-oxide-*N*′-hydroxylate) are characterized by single-crystal X-ray diffraction. From the metathesis reaction of the silver salt of methanetris(diazene-*N*-oxide-*N*′-hydroxylate) with ammonium iodide, the corresponding ammonium salt is isolated in 59% yield, but only trace amounts of methylated products form in the reaction of the silver salt with methyl iodide. Density functional calculations (B3LYP/6-311++G**) are used to evaluate the bonding, ground-state structures, and energy landscape for the different conformers of methanetris(diazene-*N*-oxide-*N*′-hydroxylate)$^{3-}$ trianion, a new type of a molecular propeller, and its corresponding triprotonated acid.

Introduction

The fundamental reactions of nitric oxide (NO) with substrates such as aliphatic alcohols,[1] alkylamines,[2,3] phenols,[4,5] acinitromethane anions,[6,7] and so forth are of considerable current interest in light of the recent discovery of nitric oxide's pervasive and numerous biological roles.[8] Being both a weak electrophile and nucleophile, nitric oxide's reactivity frequently involves one-electron transfer mechanisms, and this complication may have not only discouraged systematic mechanistic studies of its reaction chemistry, but it may also have precluded systematic studies of its reactions with organic substrates.

In a landmark paper a century ago, Traube described reactions of nitric oxide with several organic substrates containing acidic protons.[9] The products, termed isonitramines by Traube, were shown to contain one or two $N_2O_2^-$ substituents and to undergo exothermic decomposition on heating. Although Traube originally formulated the structures as **A**, the general structural features of some of the products have been well studied[10,11] and are correctly known to be acyclic, structure **B**, originally suggested by A. v. Baeyer.[12] Unfortunately, the mechanistic

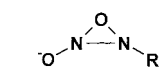

A Traube's Isonitramine Formulation

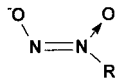

B Baeyer's Acyclic Formulation

aspects and the generality of the reactions have received only scant attention, as have the properties of the products. Traube[9] and George et al.[13] have postulated that the reaction of nitric

(1) Grossi, L.; Strazzari, S. *J. Org. Chem.* **1999**, *64*, 8076−8079.
(2) Drago, R. S.; Paulik, F. E. *J. Am. Chem. Soc.* **1960**, *82*, 96−98.
(3) Maragos, C. M.; Morley, D.; Wink, D. A.; Dunams, T. M.; Saavedra, J. E.; Hoffman, A.; Bove, A. A.; Isaac, L.; Hrabie, J. A.; Keefer, L. K. *J. Med. Chem.* **1991**, *34*, 3242−3247.
(4) Wilcox, A. L.; Janzen, E. G. *J. Chem. Soc., Chem. Commun.* **1993**, 1377−1379.
(5) Janzen, E. G.; Wilcox, A. L.; Manoharan, V. *J. Org. Chem.* **1993**, *58*, 3597−3599.
(6) Reszka, K. J.; Chignell, C. F.; Bilski, P. *J. Am. Chem. Soc.* **1994**, *116*, 4119−4120.
(7) Reszka, K. J.; Bilski, P.; Chignell, C. F. *J. Am. Chem. Soc.* **1996**, *118*, 8719−8720.
(8) Moncada, S.; Palmer, R. M. J.; Higgs, E. A. *Pharmacol. Rev.* **1991**, *43*, 109−142.
(9) Traube, W. *Justus Liebigs Ann. Chem.* **1898**, *300*, 81−128.
(10) Bryden, J. H. *Acta Crystallogr.* **1959**, *12*, 581−585.
(11) Cherepinskii-Malov, V. D.; Mukhametzyanov, A. S.; Andrianov, V. G.; Marchenko, G. A. *Russ. J. Org. Chem.* **1983**, *24*, 157−158.
(12) Baeyer, A. v. *Ber. Dtsch. Chem. Ges.* **1895**, *28*, 639−652.

10.1021/ja002634b CCC: $20.00
Published on Web 10/13/2001

oxide with acetone may involve the formation of $CH_3COCH(N_2O_2Na)_2$ as an intermediate (eq 1), though no evidence has been presented to support this hypothesis.

$$(CH_3)_2CO \xrightarrow[2NaOH/MeOH]{4NO} \text{“}CH_3COCH(N_2O_2Na)_2\text{”} \xrightarrow[H_2O]{NaOH} CH_2(N_2O_2Na)_2 + CH_3COONa \quad (1)$$

The contrast of the physical characteristics of the known alkylated diazene-*N*-oxide-*N*′-hydroxylates, RN(O)═NOR′, with the much more extensive family of nitroalkanes, RNO_2, is illustrative of their common properties and rationalizes Traube's original isonitramine terminology. Both groups are markedly electron withdrawing, with the α-hydrogens being relatively strong C−H acids, with the nitroalkanes having pK_a's at least 3 units less than those for the alkylated diazene-*N*-oxide-*N*′-hydroxylates.[14] However, unlike the nitroalkanes, which form stable nitroalkanate anions, anions derived from alkylated diazene-*N*-oxide-*N*′-hydroxylates have not been isolated. Both families of compounds have properties sought in high energy dense materials and in new propellants.

As part of our research directed toward the synthesis of nitric oxide derived propellants, we are interested in Traube's reaction, eq 1. We have observed the formation of new products from some of Traube's reactions together with the previously described products, under slightly modified reaction conditions. Therefore, we decided to examine the base promoted reaction of nitric oxide with acetone and 3,3-dimethylbutan-2-one (pinacolone). 3,3-Dimethylbutan-2-one is an appropriate choice for this study because it contains only one active methyl group in which nitric oxide addition can occur. In this paper, we report: (i) our results of the reactions of the two ketones with nitric oxide in the presence of sodium, potassium, and lithium hydroxides in methanol solution, (ii) a reaction mechanism based on the products isolated, (iii) the characterization and thermal decomposition properties of the products, and (iv) theoretical demonstration that the new tris(diazene-*N*-oxide-*N*′-hydroxylate) methanes behave as molecular propellers with correlated rotation around the C−N bonds.

Results and Discussion

The precipitated crude product obtained from the reaction of acetone with nitric oxide in a freshly prepared solution of sodium ethoxide at room temperature contains significant amounts of a product other than Traube's salt, sodium methane-1,1-bis(diazene-*N*-oxide-*N*′-hydroxylate), $CH_2(N_2O_2Na)_2$, **1**. Subsequent experiments revealed that the reaction is equally efficacious when sodium hydroxide is used in place of sodium ethoxide. Because it has been observed by MacDonald and Masson[15] that ethanol by itself undergoes reaction with nitric oxide in the presence of sodium methoxide, forming **1** and sodium formate, we prefer methanol as the solvent for the reactions. Under the experimental conditions used, there is no detectable reaction of sodium methoxide with nitric oxide.

In all of these reactions, nitric oxide is in excess, and the products formed depend markedly on the stoichiometry of substrate to base, the temperature, and the time of the transformation. Optimizing these parameters has led to the syntheses detailed in the Experimental Section. In general, the use of acetone/base ratios of 1:3 results in salts of methane-1,1-bis(diazene-*N*-oxide-*N*′-hydroxylate), while acetone/base ratios greater than 1:4 result in salts of the new anion methanetris(diazene-*N*-oxide-*N*′-hydroxylate), **2**. A second product, sodium acetate-2,2-bis(diazene-*N*-oxide-*N*′-hydroxylate) ($CH(N_2O_2Na)_2CO_2Na$), is formed in trace amounts from many of these transformations. This product was identified by a modification of Traube's procedure for the reaction of dimethylmalonate and nitric oxide, eq 2, and is detailed in the experimental.[16]

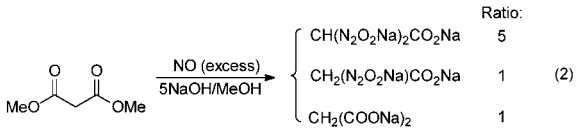

The exhaustive reaction of acetone with nitric oxide in the presence of 4 equiv of NaOH, until there is no absorption of nitric oxide (~4 d), yields **2** as the major product together with **1** (~25%) and small amounts of $CH(N_2O_2Na)_2CO_2Na$ (<1%). A similar reaction with KOH yields a mixture of products containing $CH_2(N_2O_2K)_2$, **3**, and $CH(N_2O_2K)_3$, **4**, in 6% and 36% yield, respectively. The reaction with KOH proceeds to near completion in 6 h at 0 °C yielding **4** as the major product. $CH(N_2O_2K)_2CO_2K$ is also formed in very small amounts (<1%) on the basis of the ^{1}H NMR spectrum of the crude product. A similar reaction with LiOH or MeOLi in methanol at room temperature, however, does not yield the lithium salt, $CH(N_2O_2Li)_3$, but instead yields $CH_2(N_2O_2Li)_2$, **5**, as the sole $N_2O_2^-$ containing product.

$$(CH_3)_3CC(O)CH_3 \xrightarrow[3MOH/MeOH]{6NO} (CH_3)_3CC(O)C(N_2O_2M)_3 \quad (3)$$
$$M = Na\ (\mathbf{6}),\ K\ (\mathbf{7})$$

The reaction of nitric oxide with 3,3-dimethylbutan-2-one in the presence of NaOH and KOH yields the sodium and potassium salts of 3,3-dimethylbutan-2-one-1,1,1-tris(diazene-*N*-oxide-*N*′-hydroxylate), **6** and **7**, respectively, as shown in eq 3. A similar reaction with LiOH or MeOLi does not yield the analogous lithium salt but yields **5** as the only diazene-*N*-oxide-*N*′-hydroxylate group-containing product together with lithium pivalate.

The formation of **6** and **7** in the reactions of nitric oxide with 3,3-dimethylbutan-2-one supports the sequential addition of diazene-*N*-oxide-*N*′-hydroxylate to the active methyl groups, as originally suggested by Traube and George et al.[9,13,17] Reactions of nitric oxide with sulfite in aqueous media[18−20] and those with secondary alkylamines in THF or diethyl ether[2,3,21] also yield $N_2O_2^-$ group-containing products. In these reactions, electrophilic addition of nitric oxide to incipient or latent nucleophiles is suggested to occur as the first step followed by a rapid addition of nitric oxide to the radical anion.[2,19] A similar addition of nitric oxide to ketoenolate anions, eq 4, is expected in these reactions.

$$CH_3C(O)CH_2^- \xrightarrow{NO} [CH_3C(O)CH_2NO]^{\bullet -} \xrightarrow{NO} [CH_3C(O)CH_2N_2O_2]^- \quad (4)$$

The formation of various products in the reactions described above suggests that the addition of nitric oxide depends on the

(13) George, M. V.; Kierstead, R. W.; Wright, G. F. *Can. J. Chem.* **1959**, *37*, 679−699.
(14) Woodward, R. B.; Wintner, C. *Tetrahedron Lett.* **1969**, 2689−2692.
(15) MacDonald, G. W.; Masson, O. *J. Chem. Soc.* **1894**, 944−949.
(16) Traube, W. *Ber. Dtsch. Chem. Ges.* **1895**, *28*, 1785−1797.
(17) Traube, W. *Ber.* **1894**, *27*, 1507−1510.
(18) Pelouze, J. *Ann. Pharm. (Lemgo, Ger.)* **1835**, *15*, 240.
(19) Drago, R. S. *J. Am. Chem. Soc.* **1957**, *79*, 2049−2050.
(20) Reglinski, J.; Armstrong, D. R.; Sealy, K.; Spicer, M. D. *Inorg. Chem.* **1999**, *38*, 733−737.

Scheme 1

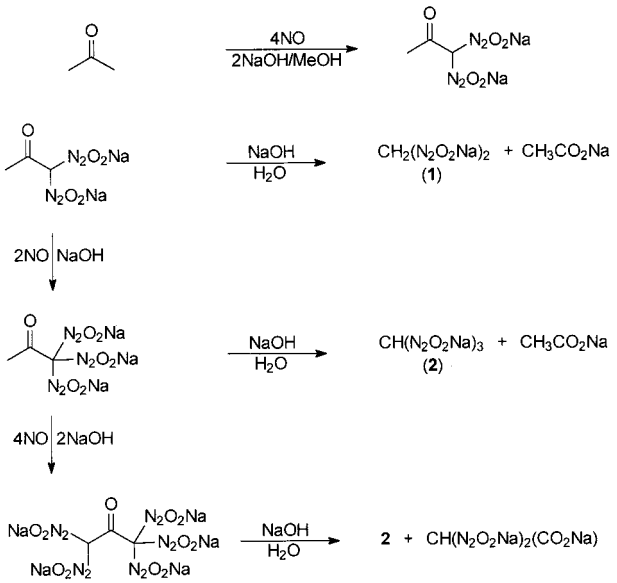

nature of the bases employed and the stability of the mono-, bis-, and tris(diazene-*N*-oxide-*N*′-hydroxylated) product formed toward hydrolytic cleavage of the C−C bond between the carbonyl and the $N_2O_2^-$ substituted carbon atoms.

Independent reactions of suspensions of bis(diazene-*N*-oxide-*N*′-hydroxylate) salts **1** and **3** with nitric oxide in methanol do not yield the corresponding tris(diazene-*N*-oxide-*N*′-hydroxylate) salts, demonstrating that $CH_2(N_2O_2)_2^{2-}$ is not an intermediate in the formation of $CH(N_2O_2)_3^{3-}$. Therefore, we propose that $CH_3COCH(N_2O_2Na)_2$ and $CH_3COC(N_2O_2Na)_3$ are intermediates, as illustrated in Scheme 1. The two intermediates are likely to be more readily hydrolyzed than the trimethylacetyl substituted methanetris(diazene-*N*-oxide-*N*′-hydroxylate) **7**, because of the absence of sterically demanding methyl substituents. In other words, the $N_2O_2^-$ substitution reaction of acetone competes with hydrolytic reactions of the bis- and tris(diazene-*N*-oxide-*N*′-hydroxylate) intermediates. The formation of $CH(N_2O_2Na)_2CO_2Na$ in less than 1% yield is also consistent with the mechanism proposed, as the tris(diazene-*N*-oxide-*N*′-hydroxylate) substituted acetone could further react with nitric oxide forming $CH(N_2O_2Na)_2COC(N_2O_2Na)_3$, which on hydrolysis could yield $CH(N_2O_2Na)_2CO_2Na$ together with **2** as shown in Scheme 1.

The formation of tris(diazene-*N*-oxide-*N*′-hydroxylate) products **2** and **4** as the major products in the reactions with NaOH and KOH in methanol and the formation of the methane bis(diazene-*N*-oxide-*N*′-hydroxylate), **5**·$2H_2O$, in the reaction with MeOLi as the only diazene-*N*-oxide-*N*′-hydroxylate, demonstrate part of the base dependency of this reaction. As described above, similar variability is also observed in the reactions with 3,3-dimethylbutan-2-one. Deprotonation of the $[RCOCH(N_2O_2)_2]^{-2}$ intermediate could readily occur in the case of strongly basic MeOK and MeONa, whereas the competing solvolysis might be more favored in the case of moderately basic MeOLi.[22] However, kinetic control of the product distribution can also result from their differing nucleophilicities.

The new products, **2**·$3^1/_2H_2O$, **4**, **5**·$2H_2O$, **6**·MeOH·H_2O, and **7**·$3H_2O$ have been characterized by NMR data, UV−vis and IR spectral data, and elemental analysis. Full spectroscopic data for previously synthesized salts **1** and **2** are included here for the first time and for comparison with the new compounds. Compound **4** and its dihydrate, **4a**, have also been characterized by single-crystal X-ray diffraction data.

Spectroscopy and Reactivity Patterns. The IR spectra of products **1**−**8** have numerous bands between 1410 and 1150 cm^{-1} due to the $N_2O_2^-$ group. The spectra of **2**·$3^1/_2H_2O$ and **4** exhibit sharp peaks at 2992 cm^{-1} associated with the C−H vibration, which are useful in distinguishing them from the corresponding methanebis(diazene-*N*-oxide-*N*′-hydroxylate) compounds **1** and **3**. In the spectrum of the deuterated analogue of **4**, the peak at 2992 is shifted to 2214 cm^{-1}, a value close to 2196 cm^{-1}, calculated from a simple harmonic oscillator model. The spectra of compounds **6**·MeOH·H_2O and **7**·$3H_2O$ exhibit a strong absorption at 1700 and 1705 cm^{-1}, respectively, clearly indicating the presence of a ketonic carbonyl group in their structure. In general, the ^1H and ^{13}C NMR spectra for the new compounds are dominated by sharp singlets with no evidence for exchange broadening, temperature dependence, or isomerism. This observation has important implications for the conformational dynamics of the trianions. This subject will be taken up below.

The UV−vis spectra of the salts of $[CH(N_2O_2)_3]^{3-}$ (**2**·$3^1/_2H_2O$ and **4**) exhibit strong absorption bands at 264 nm in aqueous alkali hydroxide solution. On the other hand, the spectra of the salts of $[Me_3CCOCH(N_2O_2)_3]^{3-}$ (**6**·MeOH·H_2O and **7**·$3H_2O$) exhibit bands at 268 nm. The spectra measured for **2**·$3^1/_2H_2O$, **4**, **6**·MeOH·H_2O, and **7**·$3H_2O$ in water exhibit a steady decay of the peaks at 264 or 268 nm and growth of another peak at 328 nm over a period of several hours. The decomposition is rapid for **6**·MeOH·H_2O and **7**·$3H_2O$ and is significantly slower for **2**·$3^1/_2H_2O$ and **4**. The formation of pivalic acid in the decomposition of **6**·MeOH·H_2O and **7**·$3H_2O$ has been established from ^1H NMR spectral studies; however, the rest of the products and those from the decomposition of **2**·$3^1/_2H_2O$ and **4** in aqueous media have not been isolated. However, on the basis of the observed similarity in the UV−vis spectra of the product and oximes, we speculate that $[HON{=}C(N_2O_2)_2]^{2-}$ results from the formal loss of one nitroxyl, NO^-, species per each anionic species. These decompositions are usually accompanied by the formation of a colorless gas, which was identified by IR spectroscopy to be nitrous oxide, the frequently observed product of putative nitroxyl dimerization in water. The decomposition behavior of the present compounds differs from those reported for dialkylamine(diazene-*N*-oxide-*N*′-hydroxylate) salts, which have been shown to release 2 equiv of nitric oxide in aqueous media,[23] but is similar to those of Angeli's salt ($Na_2N_2O_3$)[24,25] and Piloty's acid ($PhSO_2NHOH$),[26] which are thought to undergo decomposition under various conditions to give nitroxyl.

The rate of decomposition of **4** in an aqueous buffer (pH 6.6) at 25 °C was determined by measuring the decay of the peak at 264 nm. The proposed decomposition process is shown in eq 5, and the rate law for the decomposition is shown in eq 6. Under similar pH conditions, both **6**·MeOH·H_2O and **7**·$3H_2O$ undergo instantaneous decomposition.

$$CH(N_2O_2)_3^{3-} \xrightarrow{k} HON{=}C(N_2O_2)_2^{2-} + NO^- \qquad (5)$$

$$-d[CH(N_2O_2)_3^{3-}]/dt = k[CH(N_2O_2)^{3-}]$$

$$k = 2.38 \pm 0.03 \times 10^{-4}\ s^{-1} \qquad (6)$$

The UV−vis spectrum of **5**·$2H_2O$ exhibits a peak at 257 nm, the intensity of which remains unchanged over a period of

(21) Drago, R. S.; Karstetter, B. R. *J. Am. Chem. Soc.* **1961**, *83*, 1819−1822.

(22) Trotman-Dickenson, A. F. *Comprehensive Inorganic Chemistry*; Pergamon Press: Oxford, 1973; Vol. 1, p 423.

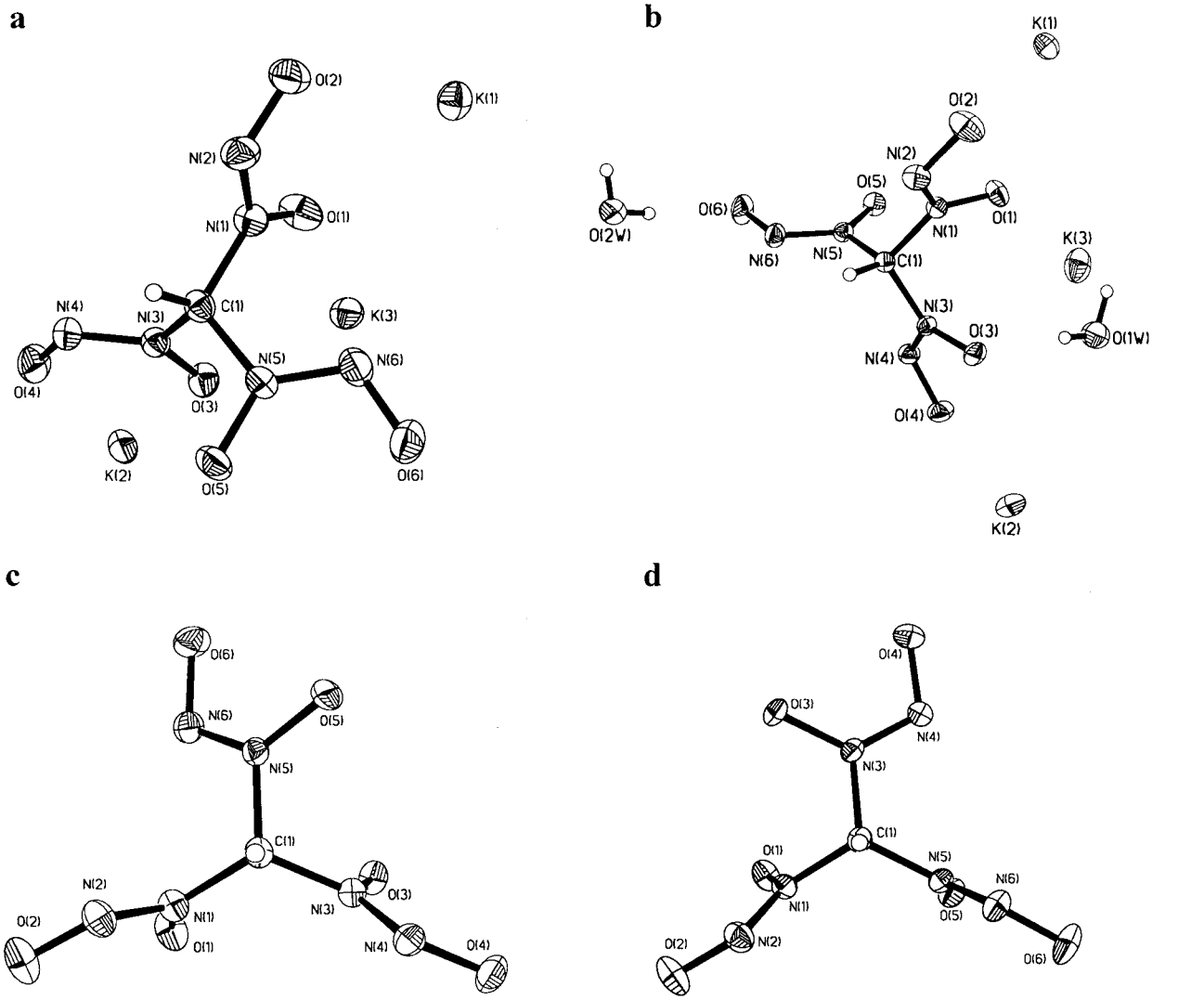

Figure 1. ORTEP representations of tripotassium methanetris(diazene-*N*-oxide-*N*′-hydroxylate) as the anhydrous form, **4** (a and c), and as the dihydrate, **4a** (b and d). Views c and d are along the H−C axes of the anions. In c, which has a clockwise helicity, N(1), N(2), N(3), and N(4) all define N_2O_2 groups with the U configuration, while N(5) and N(6) have the D configuration. In d, the helicity is counterclockwise, and N(1), N(2), N(5), and N(6) are U while N(3) and N(4) are D.

several hours, which is consistent with its stability in aqueous media similar to those of the sodium and potassium salts of $[CH_2(N_2O_2)_2]^{2-}$, **1** and **3**, respectively. The single absorption observed for all the compounds can be attributed to the $\pi \rightarrow \pi^*$ transition of the $N_2O_2^-$ group.[27] The shift of the absorption to lower energies in the case of the tris(diazene-*N*-oxide-*N*′-hydroxylate) substituted compounds in comparison to the absorption of the bis(diazene-*N*-oxide-*N*′-hydroxylate) substituted compounds is consistent with Stark effect observed for compounds containing several anionic groups.[28]

Structural Characterization of New Trianions. The solid-state structures of anhydrous **4** and its dihydrate, **4a**, have been determined by single crystal X-ray diffraction. As depicted in Figure 1a,b, each structure has nearly planar $N_2O_2^-$ groups arranged as blades of a propeller around the main C−H axis. The three blades have similar helicities, or relative orientations. Helicity can be viewed as the relative orientation of the oxygen of the carbon bound nitrogen with respect to the plane defined by the HCN atoms for the individual blades. For example, in Figure 1c, all O atoms are counterclockwise with respect to these planes. However, they typically have variable pitch or deviation from coplanarity with the defining H−C−N planes. Views along the H−C axes, shown in Figure 1c,d, illustrate the different helicities present in these two conformations, and although both individual representations in Figure 1 are chiral, crystallographic inversion symmetry relates these to their enantiomer, also present in the lattice. In addition to the chirality present in these conformations, the blades can adopt an "up" orientation (U) for the N−N bond being above the plane defined by the three carbon bound nitrogens, or below this plane with a "down" orientation (D), as shown.

In both structures, the $N_2O_2^-$ groups adopt up−up−down (UUD) conformations with their defining dihedral angles being H−C−N−N and H−C−N−O, which are useful for describing their twist around the C−N single bonds, Table 1. The other

(23) Saavedra, J. E.; Dunams, T. M.; Flippen-Anderson, J. L.; Keefer, L. K. *J. Org. Chem.* **1992**, *57*, 6134−6138.
(24) Hughes, M. N. *Q. Rev.* **1968**, *22*, 1−13.
(25) Hughes, M. N.; Wimbledon, P. E. *J. Chem. Soc., Dalton Trans.* **1976**, 703−707.
(26) Fukuto, J. M.; Hszieh, R.; Gulati, P.; Chiang, K. T.; Nagasawa, H. T. *Biochem. Biophys. Res. Commun.* **1992**, *187*, 1367−1373.
(27) Keefer, L. K.; Flippen-Anderson, J. L.; George, C.; Shanklin, A. P.; Dunams, T. M.; Christodoulou, D.; Saavedra, J. E.; Sagan, E. S.; Bohle, D. S. *Nitric Oxide* **2001**, in press.
(28) Druzhinin, S. I.; Bursulaya, B. D.; Uzhinov, B. M. *Chem. Phys.* **1991**, *158*, 137−142.

Table 1. Experimental (X-ray Diffraction) and Calculated[a] Metric Parameters for **4**, **4a**, and UUD $[HC(N_2O_2)_3]^{3-}$

Bond Length (Å)			
	X-ray diffraction		theory
parameter class[b]	**4**	**4a**	UUD-$[HC(N_2O_2)_3]^{3-}$
H−C			1.0828
C−N	1.450(3), 1.465(2), 1.460(3)	1.457(2), 1.453(2), 1.466(2)	1.4937, 1.4910, 1.4890
N−N	1.300(2), 1.300(2), 1.295(2)	1.305(2), 1.298(2), 1.291(2)	1.3149, 1.3193, 1.3004
$N_\alpha-O_\alpha$	1.295(2), 1.302(2), 1.304(2)	1.303(2), 1.314(2), 1.318(2)	1.2855, 1.2848, 1.3087
$N_\beta-O_\beta$	1.272(2), 1.281(2), 1.289(3)	1.279(2), 1.279(2), 1.282(2)	1.2885, 1.2876, 1.2864

Bond and Dihedral Angle (deg)			
parameter class[b]	X-ray diffraction		theory
	4	**4a**	UUD- $[HC(N_2O_2)_3]^{3-}$
H−C−N			105.57, 105.05, 104.49
C−N−N	112.2(2), 112.7(2), 119.0(2)	113.3(1), 112.9(1), 118.3(1)	111.59, 110.79, 118.81
$C-N_\alpha-O_\alpha$	122.3(2), 120.6(2), 114.4(2)	120.4(1), 121.4(1), 115.3(1)	121.72, 122.92, 114.29
$N_\beta-N_\alpha-O_\alpha$	125.4(2), 126.6(2), 126.5(2)	126.2(1), 125.8(1), 125.7(1)	126.19, 126.67, 126.73
$N_\alpha-N_\beta-O_\beta$	114.4(2), 114.3(2), 113.2(2)	113.4(1), 113.6(1), 113.6(1)	115.96, 115.84, 115.57
$H-C-N_\alpha-N_\beta$	16.8, 11.5, −120.9	4.5, 11.1, −101.6	15.98, 17.34, −135.49

[a] Theory level and basis set: B3LYP/6-311++G**. [b] Values for all three related parameters listed for two up (U) N_2O_2 blades followed by the value for the down (D) blade. $N_\alpha-O_\alpha$ corresponds to N(1)−O(1), N(3)−O(3), and N(5)−O(5), while $N_\beta-O_\beta$ correspond to N(2)−O(2), N(4)−O(4), and N(6)−O(6).

three possible conformations, all up, UUU, all down, DDD, and up−down−down, UDD, have not been observed. Clearly, there is a rich dynamic stereochemistry for these trianions, and the predicted energy landscape for their interconversion will be described in the subsequent theoretical section.

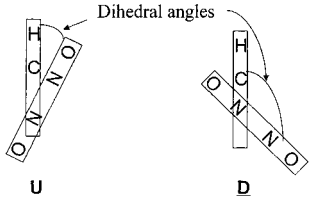

In terms of the bonding in the individual $N_2O_2^-$ groups, the observed N−N and N−O bond distances (Table 1) are in the range 1.272(2)−1.304(2) Å and lie between the ranges typically found for the corresponding single or double bonds. This is consistent with prior structural data for these groups and is also indicative of considerable electron delocalization over the four atoms, as has been found in the structures of $CH_2(N_2O_2K)_2$ and $CH_2(N_2O_2Na)_2\cdot H_2O$.[10,11] In the present structures, each of the potassium ions is surrounded by six oxygen atoms of four neighboring anions, and one or two nitrogen atoms of the neighboring anions (Figure S1, in the Supporting Information). The K−O and K−N ionic interaction leads to an infinite three-dimensional network of the ions.

Conformational Landscape of $[CH(N_2O_2)_3]^{3-}$ and $CH(N_2O_2H)_3$. Because of the observation of the UUD conformation in both crystal structures, as well as the simplicity of the ^1H and ^{13}C NMR spectra for **4** (both being sharp single peaks), we were led to consider the conformational landscape for this new trianion. In particular, we sought to determine if there is any thermodynamic stability for the UUD conformer and the barriers for its conformation interconversions. In these calculations, we utilize density functional theory, B3LYP, with large basis sets, 6-311++G**, for both the trianion and its theoretically calculated triprotonated derivative. Unlike other molecular propellers, such as the triarylmethanes with sterically demanding aryl groups,[29,30] the new derivatives have small albeit highly charged substituents. Here, Coulombic repulsion between the diazeniumdiolate groups is likely to be an important factor in determining the energy barriers for conformer interconversion.

The four ground state conformers UUU, UUD, UDD, and DDD all optimize to local minima, and their geometries, Cartesian coordinates, and vibrational frequencies are compiled in Supplementary Information (Figure S2 and Tables S1 and S2). In general, these conformations mainly differ in their H−C−N−O dihedral angles, listed in Table 2, which are all significantly greater than 0°, and thus differ in the twist of the $N_2O_2^-$ and the N_2O_2H groups with respect to the H−C−N plane. The gas-phase ground-state energies of the trianion conformations are within 1 kcal mol^{-1} of one another, Table 2, with the UUD conformer being the most stable, but only 0.063 kcal mol^{-1} more so than the UDD conformer. For the triacid, this relative ordering is reversed, but we note for both series that the UUU conformers have the highest energies, followed by the DDD conformers. In solution and/or the solid state, solvent and cation/anion interactions can thus be expected to have significant effects upon the relative stabilities of these conformers because of their differential polarities and abilities to pack into a lattice.

To illustrate the surprising energy barriers for conversion, we consider the conversion of the solid-state UUD conformation to the UDD conformation. This can be accomplished by rotation of a single U oriented $N_2O_2^-$ group around the C−N. The calculated potential energy scan of this reaction coordinate, shown in Figure 2, has a remarkably high barrier of 19.8 kcal mol^{-1}. This barrier is diminished to 7.6 kcal mol^{-1} if the two stationary $N_2O_2^-$ blades are swung out of their ground-state twisted positions, to H−C−N−O = 0°, but it still remains surprisingly high. These types of conformational reaction coordinates would predict relatively slow exchange dynamics on the NMR time scale, and this is not observed. A more realistic depiction of the conformational energy landscape is shown in Figure 3, which is a pair of plots for the calculated energies of $[CH(N_2O_2)_3]^{3-}$ as a function of the dihedral angles for $N_2O_2^-$ groups 2 and 3, while that of $N_2O_2^-$ group 1 remains at either H−C−N−O = 0°, Figure 3a, or at the observed ground-state dihedral angle, H−C−N−O = 11.5°, Figure 3b. In both cases, relatively low barriers, less than 7 kcal mol^{-1}, are predicted for either the UUU → UDU or UDU → UDD

(29) Gust, D. *J. Am. Chem. Soc.* **1977**, *99*, 6980−6982.
(30) Mislow, K. *Acc. Chem. Res.* **1976**, *9*, 26−33.

Table 2. Calculated (B3LYp/6-311++G**) Energies and Geometries for $[HC(N_2O_2)_3]^{-3}$ and $[HC(N_2O_2H)_3]$[a]

conformer	energy (AU)	relative energy (kcal mol^{-1})	H−C−N−N dihedral angles (°)
	ground state[b]		
UUU	−818.257 997 091	0.45	18.00
	(−820.202 019 527)	(1.46)	(18.00)
UUD	−818.258 097 437	0	17.34, 15.98, −135.49
	(−820.204 066 135)	(0.18)	(19.98, 17.48,−122.06)
UDD	−818.257 997 091	0.06	16.75, −137.34, −144.17
	(−820.204 350 550)	(0)	(20.72, −131.56, −142.59)
DDD	−818.257 180 560	0.13	−145.05
	(−820.203 957 563)	(0.25)	(−142.28)
	racemization transition state[c]		
UUU/*UUU*	−818.256 661 646	0.90	0
	(−820.196 986 4)	(1.46)	(0)
UUD/*UUD*	−818.255 779 252	1.45	0, 0, −180
	(−820.198 915 2)	(3.20)	(0, 0, −180)
UDD/*UDD*	−818.252 744 932	3.36	0, −180, −180
	(−820.197 031 7)	(4.10)	(0, −180, −180)
DDD/*DDD*	−818.247 193 349	6.84	−180
	(−820.191 929 350)	(7.6)	(−180)
	conformational interconversion transition state[c,d]		
UUU/UUD	−818.253 380 3	3.51	8.09, 9.33, *67.01*
	(−820.201 356 710)	(1.7)	(17.71, 18.02, *63.15*)
UUD/UDD	−818.252 031 220	(3.36)	6.61, −165.27, *72.68*
	(−820.190 462 301)	(6.4)	(5.35, −130.10, *87.76*)
UDD/DDD	−818.252 031 3	(3.74)	−175.33, −168.65, *78.89*
	(−820.191 929 3)	(7.8)	(−138.31, −128.20, *87.39*)

[a] Data for trianion given in plain type while the data for the triprotonated derivative are listed in parentheses. [b] UUU and DDD conformers have a C_3 symmetric ground state which is characterized by only one H−C−N−N torsion angle. [c] Relative energies for the transition states are calculated for the lowest energy conformer on either side of the transition state. In the case of the racemization transition states, these correspond to the ground-state energy of either enantiomer. [d] Italicized dihedral angles correspond to rotating diazenium diolate blade.

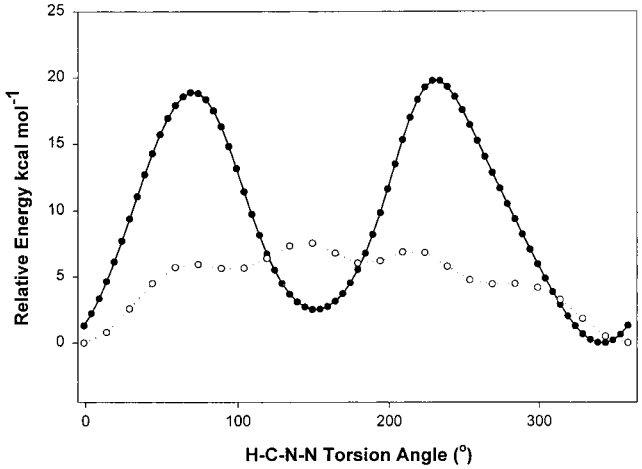

Figure 2. Calculated (B3LYP/6-311++G**) rotation barriers around a single C−N bond for the conversion of UUD to UDD $[HC(N_2O_2)_3]^{3-}$. Filled circles (●) correspond to the two unchanged blades retaining their crystallographic orientations. The open circles (○) correspond to orienting the two unchanged blades in a coplanar orientation with respect to their corresponding H−C−N planes.

interconversions. In these plots, the pathway for interconversion follows a trajectory *where both groups 2 and 3 are changing simultaneously*. That is, there is a *gearing*[31] of the motion of the propellers as they swing around their C−N axes.

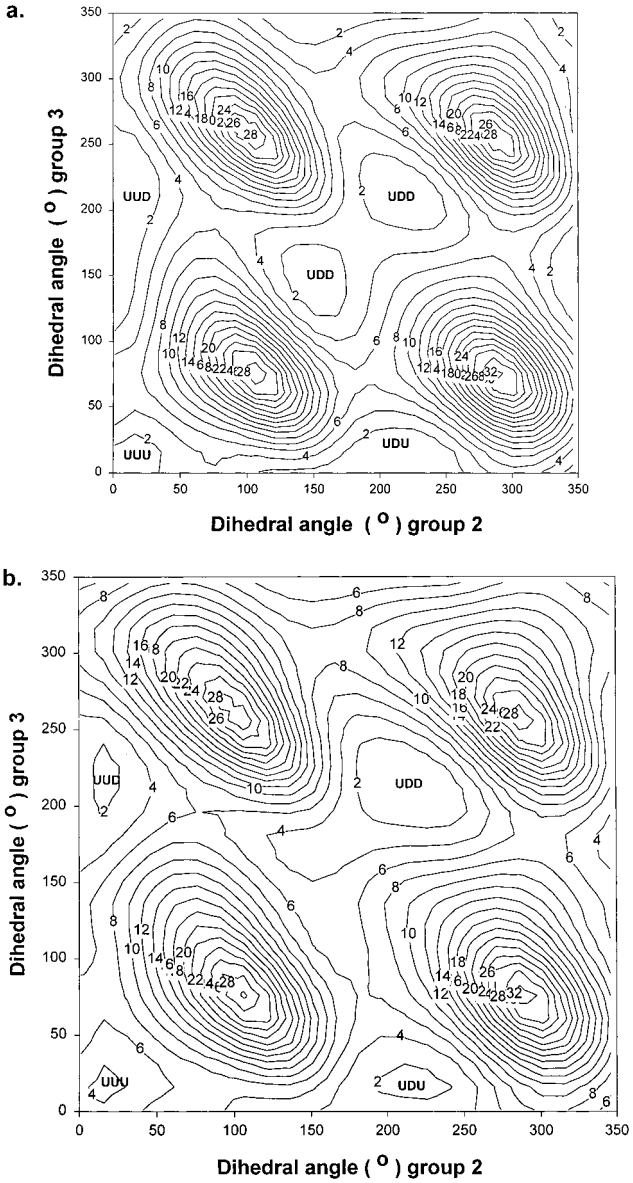

Figure 3. Calculated two-dimensional potential energy surfaces for the rotation of two of the $N_2O_2^-$ blades around their C−N bonds. Plot **a** corresponds to orienting the third $N_2O_2^-$ blade with an H−C−N−N dihedral angle of 0°, that is, coplanar with its H−C−N plane. Plot **b** corresponds to leaving this blade with its crystallographically determined dihedral angle of 11.5°. Contours correspond to 2 kcal mol^{-1} above lowest value.

A more rigorous method to estimate the energetics of these interconversions is to optimize for the saddle points separating the ground states. The results of these calculations are listed in Table 2 for both the trianion and its triacid. In these cases, the optimized barriers are all much lower than those in Figures 2 and 3. This is due to a large number of other variables optimized in these calculations. The geometries for the transition states all have planar $N_2O_2^-$ blades, and the critical dihedral angles are listed in Table 2. In addition to configurational interconversion by rotation around the C−N bonds, racemization of each conformer is also possible by transition states with all H−C−N−O dihedral angles being simultaneously 0° (or 180°), that is, having all three $N_2O_2^-$ or N_2O_2H groups coplanar with their respective H−C−N planes. For these transition states, the DDD → *DDD* racemization barrier is the largest, with a calculated

(31) Mislow, K.; Gust, D.; Finocchiaro, P.; Boettcher, R. J. *Top. Curr. Chem.* **1974**, *47*, 1−28.

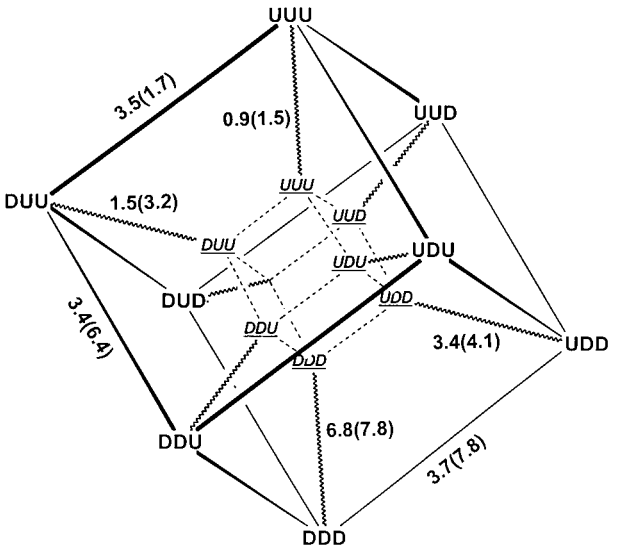

Figure 4. Graphical representation for the conformation interconversions for **4** and its corresponding triacid, $HC[N_2O_2H]_3$. Each U or D represents a single diazenium diolate blade. The outer cube represents conformers with the same helicity around the carbon, mapped with a wavy line directed to their corresponding enantiomers, *shown in underlined italics*, on the inner cube. Calculated energy barriers, B3LYP/6-311++G**, are listed for each unique conformational interconversion in kcal mol^{-1} with the value preceding the parentheses corresponding to trianion **4** and the value for $HC[N_2O_2H]_3$ within the parentheses. Similarly, the unique values for the racemization of one enantiomer to another are shown next to the corresponding wavy lines.

energy of 6.84 kcal mol^{-1}. The critical feature of all of these calculations is that low energy pathways are available for conformational interconversion and racemizations in these trianions. The graphical representation of these pathways is shown in Figure 4, where the energies are included over the tie line for each interconversion.

For the ground state conformers, the experimental and calculated bond lengths, Table 1, are in good agreement for the C—N and N═N lengths. The differences in some of the values are due to the effects of calculating the ground-state structures of a gas-phase trianion.[27] While the relative trends in N(1)—O(1) and N(2)—O(2) are correct, with the first being on average 0.019 Å longer in the X-ray diffraction structure and 0.0055 Å longer in the calculated structure, most of the difference is due to the theoretically predicted lengthening of N(1)—O(1). The concomitant buildup of charge on O(1) is mitigated by the strong cation−anion interactions in the structure of **4**. The calculated unscaled vibrational frequencies are collectively listed in the supplementary data (Table S2) and have the strongest IR bands for the $\nu(ONNO)_{sym}$ mode at 1282.2 cm^{-1}, a degenerate $\delta(CN_3) + \delta(NNO)$ combination mode at 784.6 cm^{-1}, a $\nu(ONN)_{sym}$ mode at 929.3 cm^{-1}, and the $\nu(ONN)_{asym}$ band at 834.8 cm^{-1}. In general, these bands are very sensitive to anion−cation interactions, and their energies can vary by as much as 100 cm^{-1}, depending upon whether the cation is a hydrogen bonding dialkylammonium or a coordinating alkali metal.[27] It is, therefore, not too surprising that in the tripotassium salt, **4**, the $\nu(ONNO)_{sym}$ mode is at 1360 cm^{-1} and that there are no less than three strong bands between 1279 and 1221 cm^{-1} in the IR spectrum of **4**. There is also a significant difference between the calculated and measured ν(CH) modes, 3146.7 and 2992 cm^{-1}, respectively, but this most likely reflects the differences in a gas-phase trianion versus a solid salt.

Table 3. Comparison of ^{13}C NMR Spectral Data for Mono-, Bis-, and Tris(diazene-*N*-oxide-*N*′-hydroxylate) Compounds

compound	^1H, δ, ppm	^{13}C, δ, ppm (J, Hz)	reference
$CH(N_2O_2Na)_3 \cdot 3^1/_2H_2O$[a]	7.63	99.3 (174)	this work
$CH_2(N_2O_2Na)_2 \cdot H_2O$[a]	5.93	80.5 (159)	*b*
$CH_2(N_2O_2Me)_2$ [c]	5.82	82.8 (164)	*b*
$CH_3N_2O_2Na$[a]	3.75	48.4 (143)	42

[a] In D_2O. [b] Synthesis reported in ref 9. [c] In $CDCl_3$.

Chemical Reactivity of $[CH(N_2O_2)_3]^{3-}$. The electronegative nature of the diazene-*N*-oxide-*N*′-hydroxylate substituents results in a relatively acidic methine proton in the $[CH(N_2O_2)_3]^{3-}$ anion. Consequently, the proton readily exchanges with the protons of the water solvent in aqueous solution, and the corresponding deuterium substituted salt is readily isolated by recrystallization from aqueous KOD and MeOD. The exchange is significantly faster in the presence of trace amounts of base. The hydrogen/deuterium exchange follows first-order kinetics with the rate constant, k, of 9.28×10^{-4} s^{-1} in 0.01 M KOD in D_2O. Facile hydrogen/deuterium exchange is known for $CH_2(N_2O_2Me)_2$.[14] Table 3 compares the ^1H and ^{13}C NMR data of the CH_3, CH_2, and CH groups of mono-, bis-, and tris(diazene-*N*-oxide-*N*′-hydroxylate) substituted methane compounds. Both the ^1H and ^{13}C chemical shifts exhibit a general trend of shifting downfield with an increasing number of electron withdrawing $N_2O_2^-$ groups. There is a significant increase in the value of $^1J_{CH}$ with increasing $N_2O_2^-$ substitution, and this is consistent with increasing s-orbital participation in the C—H σ-bond. Similar trends are observed for the related nitroalkanes, although the nitro group is more strongly electron withdrawing and, thus, has a more drastic effect on the pK_a of the H—C group and on its attendant $^1J_{CH}$.[32]

In general, diazene-*N*-oxide-*N*′-hydroxylate substituents are readily alkylated on either of the electron rich oxygen atoms. Traube observed the formation of two isomeric dimethyl derivatives in the reaction of silver methanebis(diazene-*N*-oxide-*N*′-hydroxylate) with methyl iodide in diethyl ether and methanol solvents.[9] Later, Woodward et al. proposed that the two isomers possess the structures shown here, and that one of them (**I**) is thermodynamically unstable whereas the other (**II**) is thermodynamically stable and chemically inert toward both strong acid and base.[14] Since this report, X-ray crystallography has confirmed the structure shown for **II**,[33] and the structure shown for **I** is consistent with NMR data for related compounds.[34]

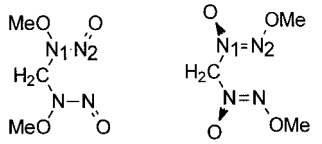

Although the methylation of $[CH(N_2O_2)_3]^{3-}$ is anticipated to result in at least two trimethyl regioisomers, rapid decomposition is observed when $[CH(N_2O_2)_3]^{3-}$ is treated with methyl iodide. For example, when a suspension of the silver salt of $[CH(N_2O_2)_3]^{3-}$ (prepared from the mixing of aqueous solutions of 3 equiv of $AgNO_3$ and 1 equiv of the sodium or potassium salt of $[CH(N_2O_2)_3]^{3-}$) in either diethyl ether or methanol is treated with 3 equiv of methyl iodide, there is vigorous generation of

(32) Reutov, O. A.; Beletskaya, I. P.; Butin, K. P. *CH-Acids*; Pergamon Press: Oxford, 1978.
(33) Cherepinskii-Malov, V. D.; Marchenko, G. A.; Mukhametzyanov, A. S.; Buzykin, B. I. *Russ. Chem. Bull.* **1985**, 871.
(34) Bohle, D. S.; Imonigie, J. A. *J. Org. Chem.* **2000**, *65*, 5685−5692.

Table 4. Differential Scanning Calorimetric Data

compd	T_{onset}, °C	T_{max}, °C	ΔH, cal/g	ΔH, kcal/mol
1·H_2O[a]	235	240	*b*	*b*
2·$3^1/_2H_2O$[a]	174	187	*b*	*b*
3	204	206	*b*	*b*
4	210	211	*b*	*b*
5·$2H_2O$	234	237	*b*	*b*
6·MeOH·H_2O[c]	134, 150, 170	145, 155, 177	−312.7	−123.89
7·$3H_2O$[c]	128, 180, 194	143, 184, 200	−382.2	−171.42
8	98	105	−200.6	−49.58

[a] An endotherm was also observed in the 95−145 °C temperature region. [b] Δ*H* values could not be determined, because the samples exploded. [c] Three closely spaced exotherms were observed.

nitrous oxide, confirmed by IR, and only traces of the expected metathesis products are isolated. The products could not be separated because of the poor yield. However, the reaction of the silver salt with ammonium iodide in aqueous ammonia readily yielded the triammonium salt, $[NH_4]_3[CH(N_2O_2)_3]$ (**8**), as described in the Experimental Section. Therefore, we speculate that the occurrence of preferential methylation of 1-nitroxy oxygen ($CN_1(O)=N_2-O^-$) in the case of at least one of the three $N_2O_2^-$ groups in the former reaction leads to the formation of thermodynamically unstable species similar to isomer **I**. We have recently described the mechanism for the origin of the site specific control in the alkylations of diazeniumdiolate anions.[34] Owing to the more rapid decomposition of **6**·MeOH·H_2O and **7**·$3H_2O$ in aqueous media, such reactions were not attempted with them.

Thermal Properties. The thermal decomposition properties of the new products together with those of the previously reported sodium and potassium methane-1,1-bis(diazene-*N*-oxide-*N*′-hydroxylate) salts have been characterized by differential scanning calorimetry(Table 4). Compounds **1**·H_2O−**5**·$2H_2O$ undergo violent exothermic decomposition. Sample cups are shattered even when minimal samples (1−2 mg) are used in the DSC experiments because of the explosive generation of gases. Compounds **6**·MeOH·H_2O, **7**·$3H_2O$, and **8** also undergo exothermic decomposition, but the sample cups remain intact during the experiments. The relatively mild exothermic decomposition of the latter compounds can be ascribed to the presence of the *tert*-butyl substituents or the ammonium cation. The overall exothermic decomposition properties of the salts reveal that the $N_2O_2^-$ substituent is thermally unstable and that the anionic substituent is similar to other nitroxy substituents such as nitro, nitroso, and oximino groups with respect to its thermal properties.[35,36] Although the enthalpy and thermal stability of these new derivatives are excellent for propellants, these compounds, as a class, are somewhat shock sensitive, and so they need to be handled with care, particularly when working with finely divided solids.

Conclusions. Up to six nitric oxides readily add to ketoenolates when they are treated with strong base in methanol. This sequential addition is both stereospecific, generating Z configured products, and kinetically controlled so that the choice of base and the base-to-substrate ratio can select the multiplicity of diazeniumdiolation. The isolation of salts of 3,3-dimethylbutan-2-one-1,1,1-tris(diazene-*N*-oxide-*N*′-hydroxylate) from the reactions of 3,3-dimethylbutan-2-one demonstrates the possible intermediacy of acetylmethanebis- and acetylmethanetris(diazene-*N*-oxide-*N*′-hydroxylate) species in the reaction of acetone with nitric oxide. Unlike the alkali salts of $[CH_2(N_2O_2)_2]^{2-}$, those of $[CH(N_2O_2)_3]^{3-}$ and $[Me_3CC(O)C(N_2O_2)_3]^{3-}$ undergo facile hydrolysis in aqueous media. Finally, the tris(diazene-*N*-oxide-*N*′-hydroxylates) are a new type of molecular propeller with relatively low energy barriers for rotation of the three N_2O_2 "blades" around the C−N bond. Theoretically, this is most consistent with a correlated or geared rotation of the different blades.

(35) Arulsamy, N.; Bohle, D. S.; Doletski, B. G. *Inorg. Chem.* **1999**, *38*, 2709−2715.

(36) Arulsamy, N.; Bohle, D. S. *J. Org. Chem.* **2000**, *65*, 1139−1143.

Experimental Section

General. The reagents and solvents used were reagent grade and used as supplied. The commercially available nitric oxide gas was purified by passing through a column packed with NaOH pellets. *Although we have had no unexpected explosions with these new salts, they should be handled carefully as finely divided solids because of their potential for friction or mechanical detonation.* Infrared spectra were obtained as KBr disks with a Midac FTIR spectrophotometer. Proton and ^{13}C NMR spectra were measured in D_2O containing DSS (3-trimethylsilyl-1-propane sulfonic acid sodium salt) (0.1% w/v) as the internal standard on a 400 MHz NMR instrument. UV−vis spectra were measured in water. Thermograms were obtained using a differential scanning calorimeter equipped with a cooling can for cooling measurements. Approximately 2 mg of the sample was placed in aluminum sample cups and crimped with a cover. The DSC runs were performed under a steady flow of argon gas and at the heating rate of 10 °C per min in the temperature range 25−500 °C.

Reactions with Nitric Oxide. Reactions of acetone and pinacolone with nitric oxide were performed using a medium-pressure reaction apparatus assembled as follows. An Andrews Glass Co. Lab Crest high-pressure glass reaction bottle was fitted to the ball valve adapter of a gas manifold using a coupling assembly. The gas manifold consisted of a ball valve adapter attached to a four-way adapter with all female fittings. Two of the three remaining fittings were connected to a stopcock and a safety valve (50 psi) through a pressure gauge. Teflon tubing, $^1/_4$ inch o.d., was used to inlet the gas to the reactor, and this was attached to a vacuum and nitrogen manifold so that nitrogen and nitric oxide gas introduction was controlled with a three-way adapter with stopcocks. Throughout the reactor, stainless steel couplings, adapters, and fittings were used, and seals were maintained with Viton O-rings. In a typical reaction, to a solution of alkali hydroxide (3 or 4 equiv) in methanol taken in the glass high-pressure reaction bottle was added the ketone (1 equiv). The bottle was fitted with the gas manifold, and the solution was stirred and degassed by purging the headspace with nitrogen. After purging for 15 min, the solution was pressurized with nitric oxide (35 psi) gas. The solution was repeatedly pressurized with nitric oxide for several hours at room temperature or at approximately −5 °C. After the completion of the reaction, the reaction mixture was flushed with nitrogen and filtered. The white or off-white precipitates formed were filtered and washed with methanol and dried in a vacuum oven at room temperature.

$CH(N_2O_2Na)_3$·$3^1/_2H_2O$ (2·$3^1/_2H_2O$). To a solution of sodium hydroxide (6.0 g, 0.15 mol) in methanol (150 mL) was added acetone (2.18 g, 0.0375 mol). The solution was allowed to react with nitric oxide as described above for 4 d at 20 °C. The white precipitate formed was filtered, washed with methanol (50 mL), and dried. The ^1H NMR spectrum of the crude product (9.5 g) indicated that it contained $CH(N_2O_2Na)_3$ together with $CH_2(N_2O_2Na)_2$ in a ∼4:1 ratio together with trace amounts of $CH(CO_2Na)(N_2O_2Na)_2$. The product was dissolved in aqueous NaOH (0.1 M, 100 mL). Methanol (20 mL) was added to the solution until the solution became cloudy. Within 2 h, colorless crystals of hydrated $CH(N_2O_2Na)_3$ began to separate from the solution. The crystals were filtered after 6 h and dried at reduced pressure at room temperature. Yield: 7.5 g (61%) based on the amount of NaOH used and assuming that 1 equiv of CH_3COONa is formed during the formation of each equiv of the two major products. Anal. Calcd for $CHN_6O_6Na_3$·$3^1/_2H_2O$: C, 3.69; H, 2.48; N, 25.85. Found: C, 3.78; H, 2.49; N, 25.64. IR (cm^{-1}): 3550−3340 b, 2992 m, 2948 m, 1651 m, 1408 m, 1382 s, 1371 s, 1338 w, 1318 w, 1289 s, 1245 s, 1193 s, 1152 w, 788 m, 955 s, 853 m, 829 s, 786 s, 668 w, 573 w. ^1H NMR: δ 7.63 s. ^{13}C NMR: δ 99.3 ($^1J_{CH}$ = 174 Hz). UV−vis: λ_{max}, 264 nm; ϵ_{max}, 20 820 $M^{-1}cm^{-1}$ in aqueous NaOH (0.1 M).

Subsequent addition of methanol (50 mL) to the filtrate led to the crystallization of $CH_2(N_2O_2Na)_2 \cdot H_2O$ (**1**·H_2O) together with small amounts of **2**·$3^1/_2H_2O$. Further recrystallization of the crystals from water yielded analytically pure **1**·H_2O. Yield: 1.20 g, 16%. Anal. Calcd for $CH_4N_4O_5Na_2$: C, 6.06; H, 2.04; N, 28.29. Found: C, 6.14; H, 1.97; N, 28.22. ^{1}H NMR: δ 5.93 s. ^{13}C NMR: δ 80.5 ($^1J_{CH}$ = 159 Hz). IR (cm^{-1}): 3490 b, 3330 b, 3260 m, 3039 m, 2981 m, 1660 m, 1598 w, 1432 m, 1415 m, 1375 s, 1351 m, 1282 m, 1261 s, 1243 s, 1152 m, 996 m, 968 s, 950 s, 778 s, 738 s, 678 w, 585 m, 546 m, 498 m. UV−vis: λ_{max}, 257 nm; ϵ_{max}, 16 850 M^{-1}cm^{-1} in water.

$CH(N_2O_2Na)_2CO_2Na \cdot 2H_2O$. To a solution of NaOH (4.0 g, 0.1 mol) in methanol (125 mL) was added dimethylmalonate (6.6 g, 0.05 mol). The solution was allowed to react with nitric oxide at room temperature for 3 d. The white precipitate that formed was filtered, washed with methanol (50 mL), and dried at reduced pressure at room temperature (6.9 g). The ^{1}H NMR spectrum of the precipitate revealed the presence of $CH(N_2O_2Na)_2CO_2Na$, $CH_2(N_2O_2Na)CO_2Na$,[37] and $CH_2(CO_2Na)_2$ in the ratio ~5:1:1. The crude product was dissolved in water (100 mL), and the solution was treated with methanol (~40 mL). On standing overnight, the cloudy solution in a closed container formed fluffy microcrystals of an unknown product (~0.5 g), which were then filtered off. The filtrate was rotary evaporated to ~20 mL at room temperature and allowed to stand at 4 °C overnight. Colorless cubic crystals of the $CH(N_2O_2Na)_2CO_2Na \cdot 2H_2O$ that formed were separated by filtration and washed with a methanol/water (50:50) solvent mixture (20 mL) and with methanol, successively. The crystals were dried at reduced pressure at room temperature. Yield: 4.35 g (31%) based on the amount of the ester used. Anal. Calcd for $C_2H_5N_4O_8Na_3$: C, 8.52; H, 1.79; N, 19.86. Found: C, 8.63; H, 1.80; N, 19.84. IR (cm^{-1}): 3600−3280 b, 2978 m, 1655−1630 s, 1419 s, 1394 s, 1374 s, 1316 s, 1262 s, 1236 s, 1202 m, 974 s, 947 s, 880 m, 830 s, 763 s, 631 m, 592 w. ^{1}H NMR: δ 6.42 s. ^{13}C NMR: δ 169.68, 91.41 ($^1J_{CH}$ = 154 Hz). UV−vis: λ_{max}, 258 nm; ϵ_{max}, 15 380 M^{-1}cm^{-1} in water.

$CH_2(N_2O_2K)_2$ (3). To a solution of KOH (5.61 g, 0.1 mol) in methanol (150 mL) was added acetone (5.8 g, 0.1 mol) with stirring. The solution was allowed to react with nitric oxide for 1 d at room temperature. The off-white precipitate formed was filtered, washed with methanol (50 mL), and dried at room temperature. The ^{1}H NMR spectrum of the crude product (7.2 g), measured immediately after dissolution in D_2O, indicated that it contained $CH_2(N_2O_2K)_2$ and $CH(N_2O_2K)_3$ in an ~8:1 ratio. The product was dissolved in water (100 mL) and allowed to evaporate slowly at room temperature in a fume hood. The solution turned yellow-brown on standing with the formation of bubbles. The off-white residue that remained after complete evaporation was dissolved in water (100 mL) and treated with methanol (50 mL). The cloudy solution was allowed to stand at room temperature for 2 d in a closed container. The colorless crystals that formed were filtered and dried at reduced pressure at room temperature. Yield: 5.3 g (56%) based on the amount of KOH used and assuming that 1 equiv of CH_3COOK is formed during the formation of each equiv of the two products. Anal. Calcd for $CH_2N_4O_4K_2$: C, 5.66; H, 0.95; N, 26.40. Found: C, 5.62; H, 1.04; N, 26.28. IR (cm^{-1}): 2984 m, 1654 w, 1429 m, 1390 s, 1318 s, 1288 s, 1234 s, 1119 w, 981 m, 948 s, 770 m, 729 s, 578 w, 498 m. ^{1}H NMR: δ 5.93 s. ^{13}C NMR: δ 80.5 ($^1J_{CH}$ = 159 Hz). UV−vis: λ_{max}, 257 nm; ϵ_{max}, 16 740 M^{-1}cm^{-1} in water.

$CH(N_2O_2K)_3$ (4). To a solution of KOH (5.61 g, 0.1 mol) in methanol (150 mL) was added acetone (5.8 g, 0.1 mol) with stirring. The solution was cooled in an ice−salt bath to approximately −5 °C and allowed to react with nitric oxide by the procedure described above for 8 h. The reaction mixture was then allowed to warm to room temperature, degassed with nitrogen, and filtered. The precipitate was recrystallized from aqueous KOH (0.1 M, 50 mL) and dimethylformamide (10 mL) as colorless crystals. Yield: 6.7 g (86%) based on the amount of KOH used and assuming 4 equiv of KOH are needed for the formation of 1 equiv of the product. Anal. Calcd for $CHN_6O_6K_3$: C, 3.87; H, 0.32; N, 27.08. Found: C, 3.88; H, 0.41; N, 26.92. IR (cm^{-1}): 2992 s, 1404 m, 1395 m, 1360 s, 1342 m, 1295 m, 1279 s, 1257 s, 1221 s, 1198 m, 1159 m, 1099 w, 1078 w, 976 m, 952 s, 945 s, 854 s, 829 s, 789 s, 574 m. ^{1}H NMR: δ 7.63 s. ^{13}C NMR: δ 99.3 ($^1J_{CH}$ = 175 Hz). UV−vis: λ_{max}, 264 nm; ϵ_{max}, 20 440 M^{-1}cm^{-1} in aqueous KOH (0.1 N).

It was also observed that the recrystallization of the crude product from aqueous KOH (0.1 M) and methanol yielded crystals of the dihydrate, **4a**. In a separate experiment conducted with similar quantities and conditions as described here, acetone and potassium hydroxide were nitrosylated in a 1:4 ratio, respectively, for two days at room temperature to give a mixture of **4** and **3** in a ratio of 4.5:1 with a total 70% yield.

$CH_2(N_2O_2Li)_2 \cdot 2H_2O$ (5·$2H_2O$). The reaction of acetone (5.8 g, 0.1 mol) in methanol containing MeOLi (2.28 g, 0.06 mol) with nitric oxide at room temperature formed an off-white precipitate over a period of 3 d. The precipitate was filtered and recrystallized from water as colorless crystals. Yield: 2.2 g (60%) based on MeOLi and assuming 3 equiv of MeOLi are needed for the formation of 1 equiv of the product. Anal. Calcd for $CH_2N_4O_6Li_2$: C, 6.53; H, 3.29; N, 30.45. Found: C, 6.64; H, 3.31; N, 30.27. IR (cm^{-1}): 3490 b, 1664 m, 1446 m, 1400 s, 1276 m, 1238 s, 1146 w, 1015 w, 985 s, 787 s, 735 s, 684 s, 693 w, 593 m, 571 m, 554 m. ^{1}H NMR: δ 5.93 s. ^{13}C NMR: δ 79.97 ($^1J_{CH}$ = 159 Hz). UV−vis: λ_{max}, 257 nm; ϵ_{max}, 16 990 M^{-1}cm^{-1} in water.

$[Me_3CCOC(N_2O_2Na)_3] \cdot MeOH \cdot H_2O$ (6·MeOH·H_2O). This compound was synthesized from the reaction of pinacolone (2 g, 0.02 mol) dissolved in methanol (50 mL) also containing NaOH (2.4 g, 0.06 mol) with nitric oxide gas by the described procedure at room temperature for 2 d. The crude product (5.4 g) contained **6** together with **1** and **2**. Solvated crystals of **6** are readily separated by recrystallization from aqueous NaOH (0.1 M, 50 mL) and methanol (10 mL) as colorless crystals. Yield: 3.1 g (41%). Anal. Calcd for $C_7H_{15}N_6O_9Na_3$: C, 21.22; H, 3.82; N, 21.21. Found: C, 21.06; H, 3.73; N, 21.36. IR (cm^{-1}): 3650−3420 b, 2976 m, 2943 m, 1700 s, 1619 w, 1372 s, 1338 w, 1300 m, 1266 m, 1206 s, 1180 m, 1059 w, 1025 w, 994 m, 944 m, 896 w, 858 s, 839 s, 793 m, 688 m, 601 w, 447 w. ^{1}H NMR (NaOD/D_2O, 0.1 M): δ 3.35 s, 1.23 s. ^{13}C NMR (NaOD/D_2O, 0.1 M): δ 202.87, 108.52, 51.71 (*C*H_3OH), 49.24, 31.50 ($^1J_{CH}$ = 128 Hz). UV−vis: λ_{max}, 268 nm; ϵ_{max}, 16 460 M^{-1}cm^{-1} in aqueous NaOH (0.1 N).

$Me_3CCOC(N_2O_2K)_3 \cdot 3H_2O$ (7·$3H_2O$). This compound was synthesized by the procedure described above for the synthesis of **6**·MeOH·H_2O using KOH in place of NaOH. The crude product (5.8 g) was recrystallized from aqueous KOH (0.1 M) and methanol as colorless crystals. Yield: 4.95 g (55%). Anal. Calcd for $C_6H_{15}N_6O_{10}K_3$: C, 16.07; H, 3.37; N, 18.73; O, 35.67. Found: C, 16.15; H, 3.28; N, 18.78. IR (cm^{-1}): 3436 b, 2996 m, 2983 m, 1705 s, 1369 s, 1302 m, 1263 w, 1217 s, 1167 m, 1068 w, 1003 w, 987 w, 941 m, 895 w, 858 s, 837 s, 789 m, 688 m, 603 w, 458 w. ^{1}H NMR (KOD/D_2O, 0.1 M): δ 1.23 s. ^{13}C NMR (KOD/D_2O, 0.1 M): δ 202.99, 108.52, 49.24, 31.49 ($^1J_{CH}$ = 127.9 Hz). UV−vis: λ_{max}, 268 nm; ϵ_{max}, 16 010 M^{-1}cm^{-1} in aqueous KOH (0.1 N).

$[NH_4]_3[CH(N_2O_2)_3]$ (8). The silver salt, $CH(N_2O_2Ag)_3$, was prepared by mixing freshly prepared aqueous solutions of $AgNO_3$ (1.53 g, 9 mmol) and $CH(N_2O_2K)_3$ (0.931 g, 3 mmol). The voluminous precipitate was filtered immediately and washed thoroughly with distilled water. The precipitate was dissolved in aqueous ammonium hydroxide (30%, 20 mL) and treated with an aqueous solution of NH_4I (1.304 g, 9 mmol) with stirring. The precipitated silver iodide was filtered off after 30 min, and the filtrate was allowed to stand overnight in a closed container. The small amount of silver iodide formed was filtered off. The filtrate was treated with methanol until cloudiness occurred. The cloudy solution was allowed to stand at ~5 °C for 3 d. The colorless crystals formed were filtered, washed with methanol (10 mL), and dried in vacuo. Yield: 0.44 g (59%). Anal. Calcd for $CH_{13}N_9O_6$: C, 4.86; H, 5.30; N, 51.00. Found: C, 4.97; H, 5.27; N, 50.73. IR (cm^{-1}): 3225 s, 3166 s, 3060 s, 2981 s, 1684 w, 1438 s, 1406 s, 1384 m, 1344 m, 1338 s, 1270 s, 1249 s, 1220 s, 1197 s, 958 m, 930 s, 851 m, 823 s, 793 s, 578 w, 525 m, 472 w. ^{1}H NMR (D_2O): δ 7.61 s. ^{13}C NMR (D_2O): δ 99.50 ($^1J_{CH}$ = 175 Hz). UV−vis: λ_{max}, 264 nm; ϵ_{max}, 17 976 M^{-1}cm^{-1} in aq KOH (0.1 N).

Kinetics. The proton/deuterium exchange rate of the methine proton in **4** was determined by measuring the intensity of the single proton peak in the NMR spectrum in 0.01 N KOD with reference to the peak intensity of an internal standard (sodium acetate). The rate of decomposition of **4** was measured on a diode array UV−vis spectrom-

(37) Arulsamy, N.; Bohle, D. S. Unpublished Data.

eter. The pH of the solution was maintained at 6.6 using Na_2HPO_4/citric acid buffer, and the temperature was maintained at 25 °C. The decomposition was monitored in the 200−400 nm wavelength region.

Ab Initio Calculations. Ground-state geometries were calculated using the *Gaussian98* program suite,[38] on a Silicon graphics Origin system. Basis sets and theoretical methods are similar to those described in prior reports; to summarize, Becke's three parameter functionals were used (B3LYP) with large basis sets (6-311++G**) in order to effectively model the charge distribution in the trianion.[39]

Crystallographic Data. X-ray diffraction data were collected for **4** and its dihydrate, **4a**, on a Siemens P4 diffractometer equipped with a molybdenum tube and a graphite monochromator with radiation, $\lambda =$ 0.710 73 Å. Single crystals of the compounds were mounted on a glass fiber using epoxy resin. Unit cell dimensions were determined from several accurately centered reflections in high 2θ angles using XSCANS program.[40] Three standard reflections measured after every 97 reflections exhibited no significant loss of intensity for any of the samples. The data, measured by ω scans at ambient temperatures, were corrected for Lorentz polarization effects and absorption. The structures were solved by direct methods and refined by least-squares techniques on F^2 using SHELXTL program.[41] All atoms were located in the difference maps during successive cycles of least-squares. The positions of the non-hydrogen atoms were refined anisotropically, whereas those of the hydrogen atoms were refined isotropically. Important crystallographic data collection and solution parameters are collected in Table 5, while critical metric parameters are listed in Table 1.

Table 5. Crystallographic Data for **4** and **4a**

	$CHK_3N_6O_6$, **4**	$CH_5K_3N_6O_8$, **4a**
fw	310.38	346.41
λ, Å	0.710 73	0.710 73
space group	*C*2/*c*	$P\bar{1}$
$\bar{a}$, Å	13.828(2)	7.636(2)
b, Å	7.3125(6)	9.3213(11)
c, Å	19.731(2)	9.422 39(17)
α, deg		63.21(2)
β, deg	107.692(6)	88.84(3)
γ, deg		72.97(2)
V, Å^3	1900.7(3)	567.5(2)
Z	8	2
μ, mm^{-1}	1.462	1.248
ρ_{calcd}, g cm^{-3}	2.169	2.027
T, °C	25	25
reflns collected	2232	2350
obsd reflns [$I > 2\sigma(I)$]	1679	1883
no. parameters	149	183
S_{GOF} on F^2	1.099	1.089
R_1 [a] [$F > 4\sigma(F)$]	0.0260	0.0234
wR_2 [b]	0.0688	0.0629

[a] $R_1 = \sum||F_o| - |F_c||/\sum|F_o|$. [b] $wR_2 = [\sum\{w(F_o^2 - F_c^2)^2\}/\sum\{w(F_o^2)^2\}]^{1/2}$.

Acknowledgment. We gratefully acknowledge financial support from the Air Force Office of Scientific Research, Grants F49620-96-1-0417 and 98-1-0461.

Supporting Information Available: Figures showing the cation environments, the calculated ground-state geometries, as well as tables of optimized ground-state geometries, and calculated vibrational frequencies for $[CH(N_2O_2)_3]^{3-}$, as well as complete X-ray crystallographic data in the form of positional parameters and anisotropic displacement parameters for **4** and **4a**. This material is available free of charge via the Internet at http://pubs.acs.org.

JA002634B

(38) Frisch, M. J.; Trucks, G. W.; Schlegel, H. B.; Scuseria, G. E.; Robb, M. A.; Cheeseman, J. R.; Zakrzewski, V. G.; Montgomery, J. A., Jr.; Stratmann, R. E.; Burant, J. C.; Dapprich, S.; Millam, J. M.; Daniels, A. D.; Kudin, K. N.; Strain, M. C.; Farkas, O.; Tomasi, J.; Barone, V.; Cossi, M.; Cammi, R.; Mennucci, B.; Pomelli, C.; Adamo, C.; Clifford, S.; Ochterski, J.; Petersson, G. A.; Ayala, P. Y.; Cui, Q.; Morokuma, K.; Malick, D. K.; Rabuck, A. D.; Raghavachari, K.; Foresman, J. B.; Cioslowski, J.; Ortiz, J. V.; Stefanov, B. B.; Liu, G.; Liashenko, A.; Piskorz, P.; Komaromi, I.; Gomperts, R.; Martin, R. L.; Fox, D. J.; Keith, T.; Al-Laham, M. A.; Peng, C. Y.; Nanayakkara, A.; Gonzalez, C.; Challacombe, M.; Gill, P. M. W.; Johnson, B. G.; Chen, W.; Wong, M. W.; Andres, J. L.; Head-Gordon, M.; Replogle, E. S.; Pople, J. A. *Gaussian 98*; Gaussian, Inc.: Pittsburgh, PA, 1998.

(39) Arulsamy, N.; Bohle, D. S.; Imonigie, J. A.; Sagan, E. *J. Am. Chem. Soc.* **2000**, *122*, 5539−5549.

(40) *XSCANS*, version 2.31; Siemens Energy and Automation, Inc.: Madison, WI, 1997.

(41) Sheldrick, G. M. *SHELXTL*, version 5.04; Siemens Energy and Automation, Inc.: Madison, WI, 1996.

(42) Zyuzin, I. N.; Lampert, D. B. *Russ. Bull. Chem.* **1984**, 753−756.